*Optica Applicata, Vol. XLII, No. 4, 2012*
DOI: 10.5277/oa120411

# Sharp transition of laser-induced periodic ripple structures

HAIFENG YANG*, HAIDONG HE, LONGPENG ZHOU, JIGUO QIAN, JINGBIN HAO, HUA ZHU

College of Mechanical and Electrical Engineering, China University of Mining and Technology, Xuzhou 221116, China

*Corresponding author: yhf002@163.com

Laser-induced periodic surface structures (LIPSS) (ripple) with different spatial frequencies have been observed after irradiation of stainless steel surfaces by femtosecond laser pulses in the air. Low spatial frequency LIPSS (LSFL) with the period (about 830 nm) close to the laser wavelength and high spatial frequency LIPSS (HSFL) with half wavelength (about 410 nm) were dependent on the scanning speed of laser focus. The sharp transition from the single LSFL to double HSFL structures occurs at 5 mm/s. This abrupt transition of dividing one ripple into two equals was proved.

Keywords: stainless steel, ripple, sharp transition, ripple equipartition.

## 1. Introduction

Periodic micro-nanostructures on materials surface have been widely applied in different technical implementations. Surface microstructures can change surface properties, such as adhesion, friction, wettability, *etc*. [1–5]. Laser-induced periodic surface structures (LIPSS) were achieved soon after the laser was invented. Meanwhile, several mechanisms were proposed to explain their formation [6]. LIPSS were obtained on various materials such as metals, semiconductors, and dielectrics [7–9]. Among them, a femtosecond laser induced periodic ripple attracted an increasing interest because it can be achieved on almost any material directly.

Most LIPSS with a period close to the laser wavelength were referred as low spatial frequency LIPSS (LSFL). Recently, several research groups reported high spatial frequency LIPSS (HSFL) with a period far less than the wavelength. Many studies of LSFL and HSFL were carried out on various materials [10–12]. For normal incident laser radiation, the LSFL with a period (630–730 nm) close to the wavelength and the HSFL with the periods between 200 and 280 nm were obtained on ZnO surfaces. A sharp transition from the LSFL features toward HSFL appears for lower fluences

(0.5–0.7 J/cm). Their experimental results proved that the surface scattered second harmonic generation (SHG) is presented in the regime of HSFL formation [12]. YANG YANG *et al*. [13] found that the ripple period increases with higher laser average fluence but reduces with a larger number of laser pulses, and the threshold fluence for the HSFL depends on the surface roughness of NiTi alloy plate. Using two classes of metallic materials (transition and noble), COLOMBIER *et al*. have determined that the ripples amplitude is strongly correlated to the material transport properties, namely electron–phonon relaxation strength, electronic diffusion, and to the energy band characteristics of the electronic laser excitation [14]. Additionally, they presented the efficiency of energy coupling in ultrashort laser-irradiated metallic surfaces with different intensity envelopes and discussed probable thermodynamic paths for material ejection under the laser action [15]. ROMER *et al*. investigated femtosecond laser induced self-organizing ripple nanostructures on steel. A low fluence results in "regular ripples" with a spatial repetition of 300–500 nm. In twinned areas "pre-ripples" with much smaller wavelength (about 150 nm) are observed [16]. VARLAMOVA *et al*. presented numerical simulations from an adopted surface erosion model and compared the result to experimental data on laser-induced nanostructures formation. Their results support the nonlinear self-organization mechanism of pattern formation on the surface of solids [17, 18]. The natures of LSFL and HSFL are still quite controversially discussed in the literature and several different mechanisms have been proposed, such as interference effects [19], second harmonic generation [10], excitation of surface plasmon polaritons [20], or self-organization [8].

Stainless steels are a kind of metallic materials used to fabricate artificial joints. In clinical practice, the stainless steel implanted in the human body will release $Cr^{3+}$, $Ni^{2+}$, and $Cr^{5+}$ in the physical environment because of its friction and wear and cause artificial joints failure ultimately [21]. Therefore, it is necessary to improve the wear resistance of stainless steel surface for prolonging the life of artificial joints. It is an effective method to improve the wear resistance by fabricating periodic nanostructures on material surface [22, 23]. For the stainless steels, there are some studies on the formation of femtosecond LIPSS. BO WU *et al*. obtained the LSFL on stainless steel surface by a femtosecond laser and achieved its superhydrophobicity [9]. LITAO QI *et al*. fabricated 526 nm LSFL and 310 nm HSFL on stainless steel surface [24]. They reported that this periodic ripple structure originated from the interference between the incident laser light and the scattered tangential wave. WEI ZHANG *et al*. found abrupt transition from wavelength structure to subwavelength structure in a single-crystal superalloy by femtosecond laser irradiation and studied the parametric dependence of this transition on fluence and pulse number [25]. However, femtosecond LIPSS on stainless steel surface still needs further study. Therefore, we experimen-talized the interaction of a focused femtosecond laser and stainless steel surface detailedly.

In this paper, we present a complementary study on the formation of LIPSS on stainless steel surface by femtosecond laser irradiation. This paper studies the depen-

dence of LSFL and HSFL formations on laser parameters (laser average fluence and scanning speed) to extend the existing works on this material. Lastly, we proved the phenomenon (Abrupt transition [25]) of the LIPSS transition from LSFL toward HSFL.

## 2. Experiment

In the experiments, the samples were AISI 316L type austenitic stainless steel plates with 0.2 mm thickness. After mechanical polishing, the $S_a$ value is about 4.26 nm measured by atomic force microscopy (SCPM 5500). Then, the samples had two 30-min ultrasonic cleanings in deionized water and in acetone, respectively.

A commercial chirped pulse amplification based Ti:sapphire regenerative amplifier laser system was used to generate linearly polarized laser pulses at 775 nm center wavelength, 150 fs pulse duration and 1 kHz repetition rate. Using a NA = 0.14, 5× objective lens, the laser pulses were focused directly onto the samples, and the laser focus was located below the stainless steel surface of 5 mm. Therefore, the beam diameter in the sample processing plane is about 150 μm. Meanwhile, the laser average fluence in the sample processing plane can be calculated. The exposure time of femtosecond laser was controlled by a fast mechanical shutter. The scanning of laser focus was achieved by three dimensional piezoelectric translation stages. All irradiations were performed in the air. Figure 1 shows the schematic diagram of the femtosecond laser processing system.

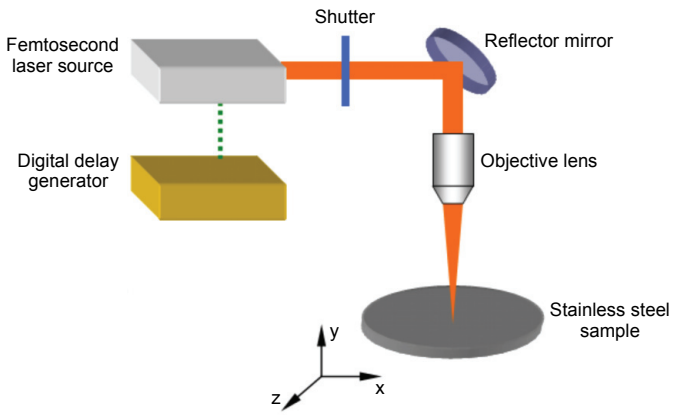


Fig. 1. Schematic diagram of femtosecond laser processing system.

Femtosecond laser was focused on the stainless steel surface through an objective lens. Meanwhile, stainless steel moved at a fixed speed through three dimensional piezoelectric translation stages to obtain one irradiated line. In order to study the laser parameters influence on the irradiated line, the scanning speeds and the laser average fluence were systematically varied. Each irradiated line was corresponding to a group of laser parameters (laser average fluence and scanning speed).

After experiments, the samples were cleaned with methanol in an ultrasonic bath. The processing morphologies were characterized by a scanning electron microscope (SEM) and atomic force microscopy (AFM). The periods of LIPSS were measured by AFM section analyzing, and the results were the average of five measured values.

## 3. Results and discussion

The phenomenon, also called abrupt transition, is observed when the stainless steel surface is irradiated by scanning femtosecond laser focus. Four irradiated lines are achieved on stainless steel surface by changing the scanning speeds (10, 5, 2, 1 mm/s) at 0.24 J/cm$^2$ laser average fluence. The average pulse numbers per beam diameter are 15, 30, 75, 150, respectively. The morphologies and ripple periods of irradiated lines are measured by SEM and AFM, respectively. Figure 2 shows the SEM micrographs of LIPSS, in which the regular ripples appeared, whose direction is perpendicularly oriented to the laser polarization.

The ripple periods of Figs. 2**a** and 2**b** are about 830 nm (close to the laser wavelength), and those of Figs. 2**c** and 2**d** are about 410 nm (close to half wavelength). When scanning speed is 10 mm/s (Fig. 2**a**), narrow ridge of ripple structures indicates that the speed is too fast. The ripple period in Fig. 2**b** (5 mm/s) is consistent with that of Fig. 2**a**, but it has wider ridge and narrower gap. It means that the ripple period is unchanged basically within 10–5 mm/s range. Besides, the bifurcation phenomenon in the middle of single ripple appears occasionally, which is marked by arrow in Fig. 2**b**. Then, AFM is adopted to further investigate the bifurcation phenomenon (as

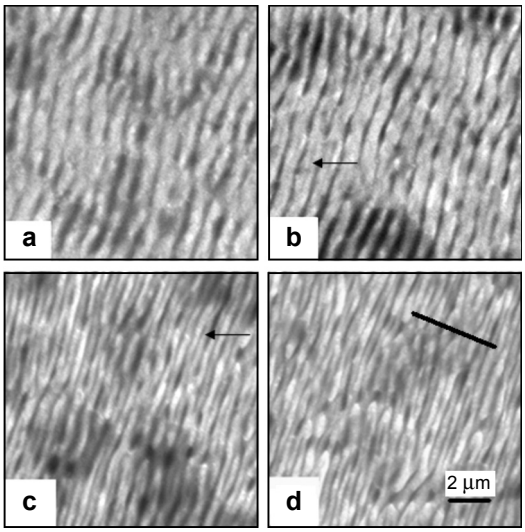


Fig. 2. SEM micrographs of structures on stainless steel surface induced by scanning femtosecond laser focus with varied speeds and fixed laser average fluence (0.24 J/cm$^2$). 10 mm/s, 15 pulses (**a**); 5 mm/s, 30 pulses (**b**); 2 mm/s, 75 pulses (**c**); 1 mm/s, 150 pulses (**d**). The black line in (**d**) represents the polarization direction.

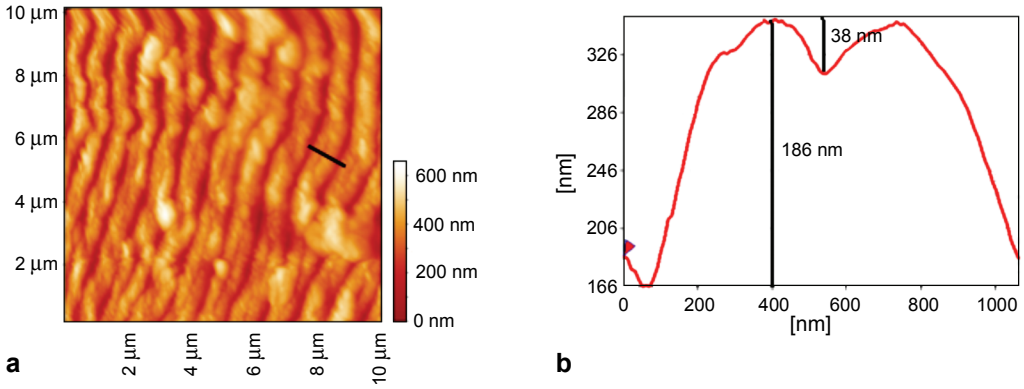


Fig. 3. AFM micrographs of ripple structure when the speed and laser average fluence are 5 mm/s (30 pulses) and 0.24 J/cm$^2$. Two-dimensional morphology (**a**), and section contour (**b**).

shown in Fig. 3). Figure 3**a** is the two-dimensional topography of local area, in which the bifurcation appears in the middle of some ripple structure distinctly. Figure 3**b** shows the section contours of Fig. 3**a** in a black line position. The depth of newly generated groove is about 38 nm, which is shallower than that of the 186 nm-groove. Maybe this represents the initial phase of the ripple structure bifurcation, namely the transition stage from LSFL to HSFL. Figure 2**c** shows the formed ripple structure at 2 mm/s scanning speed, and its period is 410 nm (close to half wavelength). These ripple structures should belong to HSFL. However, the adjacent groove depths have minor discrepancies. The arrow points to the shallow groove, and the adjacent is the deep groove. It is further demonstrated that two HSFL originate from one LSFL. This phase is considered as a developmental stage of the transition from LSFL to HSFL. When the scanning speed is 1 mm/s, the ripple period is about 410 nm, and the grooves between ripples are also uniform. This phase is considered as the completion stage of the transition from LSFL to HSFL. The ripple period after bifurcation is half as much as that of pre-bifurcation. This phenomenon is called the abrupt transition.

In order to study the transition of two ripple types and their parametric influence, the scanning speed and the laser average fluence were systematically varied. We chose four laser average fluences (0.12, 0.24, 0.45, 0.9 J/cm$^2$) and four scanning speeds (10, 5, 2, 1 mm/s) to irradiate the stainless steel surface, and obtained 16 irradiated lines, also called 16 samples. The corresponding relations between 16 laser parameters and 16 samples are listed in Table 1. After experiments, SEM and AFM are adopted to observe and measure the ripple morphology.

Three phenomena (LSFL, HSFL and ripple rupture) are found in the series of experiments. Ripples of four samples (A1, B1, C1, D1) gradually become obvious, which indicates that the ripple can even form at the high scanning speed under larger laser average fluence. Although the ripple ridge widths in four samples (A1, B1, C1, D1) are different, the ripple periods are basically around 830 nm (belonging to LSFL). Surface morphology of four samples (A2, B2, C2, D2) is also similar. Their ripple structures belong to LSFL, too. However, there are occasional ripple bifurcation

T a b l e 1. Relationship between sample and laser parameters (laser average fluence and speed).

| Samples, LSFL/HSFL | $V$ = 10 mm/s (15 pulses) | $V$ = 5 mm/s (30 pulses) | $V$ = 2 mm/s (75 pulses) | $V$ = 1 mm/s (150 pulses) |
|---|---|---|---|---|
| $P$ = 0.12 J/cm$^2$ | A1, LSFL | A2, LSFL | A3, HSFL | A4, HSFL |
| $P$ = 0.24 J/cm$^2$ | B1, LSFL | B2, LSFL | B3, HSFL | B4, HSFL |
| $P$ = 0.45 J/cm$^2$ | C1, LSFL | C2, LSFL | C3, HSFL | C4, HSFL |
| $P$ = 0.9 J/cm$^2$ | D1, LSFL | D2, LSFL | D3, HSFL | D4, HSFL |

phenomena on B2, C2, D2, which means shallow groove appears in the middle of single ripple (similar to Figs. 2**b** and 3). Ripple structures in A2 sample have no bifurcation because of lower laser average fluence. As the result of the excess laser average fluence, ripple structures in D2 sample present rupture phenomenon, and the rupture direction is perpendicular to the ripple direction. Ripple structures in four samples (A3, B3, C3, D3) all present bifurcation. However, the adjacent groove depths have minor discrepancies (similar to Fig. 2**c**). The periods of ripple structures are about 410 nm, which belong to HSFL. The four samples are all in developmental stage of the transition from LSFL to HSFL. C3 and D3 samples have the same rupture phenomenon like the sample D2. But the rupture of D3 sample is more apparent. Surface morphology of four samples numbered A4, B4, C4, D4 is similar. The bifurcation of ripple structure is basically completed, and the periods are about 410 nm, which belong to HSFL. Meanwhile, the ripples of four samples present the rupture. As the laser average fluence is increasing, the rupture is more serious. Figure 4 shows the SEM

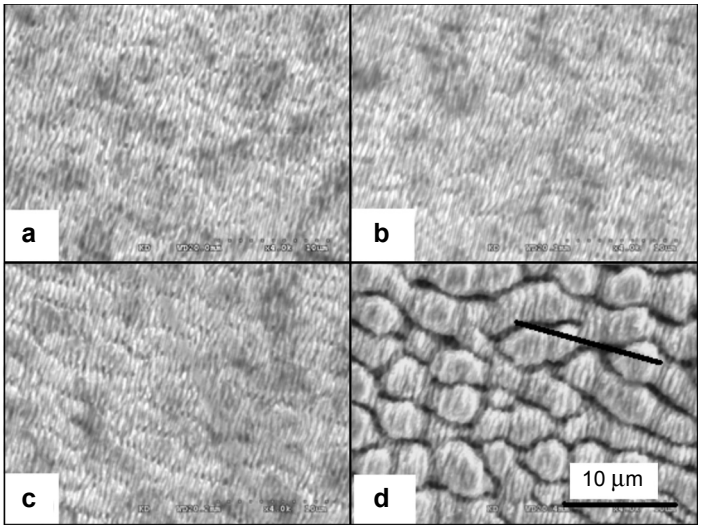


Fig. 4. SEM micrographs of structures on stainless steel surface induced by scanning femtosecond laser focus with fixed speed (1 mm/s,150 pulses) and varied laser average fluence. 0.12 J/cm$^2$ (**a**), 0.24 J/cm$^2$(**b**), 0.45 J/cm$^2$ (**c**), 0.9 J/cm$^2$ (**d**). The black line in (**d**) represents the polarization direction.

images of A4, B4, C4 and D4 samples. Through a series of experiments listed in Tab. 1, we draw the following conclusions:

– The ripple structures can form at specified scanning speed under four different laser average fluences;

– The ripple bifurcation begins to appear at the speed of 5 mm/s, more obvious at 2 mm/s, and complete at 1 mm/s;

– There are two possibilities about ripple periods, which are 830 nm LSFL and 410 nm HSFL corresponding to the state before bifurcation and after bifurcation, respectively.

– The ripple bifurcation is determined by the scanning speed and has no relation with laser average fluence;

– When laser average fluence is higher, ripple structure will rupture even at higher scanning speed. Laser average fluence only affects rupture but not period.

For the femtosecond laser irradiation on the stainless steel surface, the free electrons are quickly heated to escape from the surface through both photoelectric and thermionic emission processes, resulting in micro-scale electric plasma in close contact with the solid-state matter even during the pulse [26]. According to the previous studies [27], ripples formation originated from interference of the laser with the excited surface plasmon polariton. Accordingly, the induced ripple periodicity will be somewhat larger than the wavelength of incident lasers. The formation of LSFL on the ablated area was attributed to the interference between the incident beam and the scatter waves, which has been studied for many years. However, many scholars obtained different research results. Stoian thought that ripples growth depended on the electron–phonon coupling and electron diffusion [14]. Reif concluded that the laser polarization was a control parameter in the formation of laser-induced periodic surface structures based on their comparison of numerical and experimental results [17, 18]. The work of Sipe *et al*. [6] represented the ripple attributed to scattering from surface roughness and to the re-radiation from surface defect sites. The interference between all incident, radiated, or scattered electromagnetic fields causes periodic variation in substrate heating and ultimately the periodic surface structure. Therefore, from works above it becomes clear that interference cannot explain the observed phenomena. Interference is not generally accepted as the only theory to explain ripples. Additionally, Bonse thought that this sharp transition from the formation of HSFL to the LSFL occurs at a certain laser average fluence level [12]. In our experiment, the transition from the LSFL to HSFL depends on the scanning speed, or repetition rates of laser focus. Besides, the phenomena of one LSFL dividing into two HSFL is observed. However, the mechanism of ripple equipartition at 5 mm/s speed is unknown and needs further study.

## 4. Conclusions

In conclusion, we have performed a detailed study of the femtosecond LIPSS on stainless steel surface, which is influenced by laser parameters (laser average fluence,

and scanning speed). The phenomenon, also called abrupt transition, was observed when the stainless steel surface is irradiated by femtosecond laser. The bifurcation of ripple structure begins to appear at 5 mm/s, more obvious at 2 mm/s, and complete at 1 mm/s. There are two possibilities about the period of ripple structure, which are 830 nm LSFL and 410 nm HSFL corresponding to the state before bifurcation and after bifurcation, respectively.

*Acknowledgements* – This work was supported by the grant from Fundamental Research Funds for the Central Universities (2012QNA25) and Priority Academic Program Development of Jiangsu Higher Education Institutions.

## References

[1] YUFEI MO, YING WANG, JIBIN PU, MINGWU BAI, *Precise positioning of lubricant on a surface using the local anodic oxide method*, Langmuir **25**(1), 2009, pp. 40–42.

[2] CHEN H., GOU G.Q., TU M.J., LIU Y., *Structure and wear behaviour of nanostructured and ultrafine HVOF spraying WC-17Co coatings*, Surface Engineering **25**(7), 2009, pp. 502–506.

[3] GUERRA NETO C.L.B., DA SILVA M.A.M., ALVES C., *Experimental study of plasma nitriding dental implant surfaces*, Surface Engineering **25**(6), 2009, pp. 430–433.

[4] ZHAO B., YADIAN B.L., LI Z.J., LIU P.; ZHANG Y.F., *Improvement on wettability between carbon nanotubes and Sn*, Surface Engineering **25**(1), 2009, pp. 31–35.

[5] GOLOZAR M.A., MOSTAGHIMI J., COYLE T., *Wear behaviour of nanostructured and conventional 8 wt-%$Y_2O_3$–$ZrO_2$ coatings against $Si_3N_4$ ball*, Surface Engineering **22**(5), 2006, pp. 399–407.

[6] SIPE E., YOUNG J.F., PRESTON J.S., VAN DRIEL H.M., *Laser-induced periodic surface structure. I. Theory*, Physical Review B **27**(2), 1983, pp. 1141–1154.

[7] QUAN SUN, FENG LIANG, VALLÉE R., SEE LEANG CHIN, *Nanograting formation on the surface of silica glass by scanning focused femtosecond laser pulses*, Optics Letters **33**(22), 2008, pp. 2713–2715.

[8] LI J.M., XU J.T., *Self-organized nanostructure by a femtosecond laser on silicon*, Laser Physics **19**(1), 2009, pp. 121–124.

[9] BO WU, MING ZHOU, JIAN LI, XIA YE, GANG LI, LAN CAI, *Superhydrophobic surfaces fabricated by microstructuring of stainless steel using a femtosecond laser*, Applied Surface Science **256**(1), 2009, pp. 61–66.

[10] BONSE J., MUNZ M., STURM H., *Structure formation on the surface of indium phosphide irradiated by femtosecond laser pulses*, Journal of Applied Physics **97**(1), 2005, article 013538.

[11] HSU E.M., CRAWFORD T.H.R., MAUNDERS C., BOTTON G.A., HAUGEN H.K., *Cross-sectional study of periodic surface structures on gallium phosphide induced by ultrashort laser pulse irradiation*, Applied Physics Letters **92**(22), 2008, article 221112.

[12] DUFFT D., ROSENFELD A., DAS S.K., GRUNWALD R., BONSE J., *Femtosecond laser-induced periodic surface structures revisited: a comparative study on ZnO*, Journal of Applied Physics **105**(3), 2009, article 034908.

[13] YANG YANG, JIANJUN YANG, LU XUE, YAN GUO, *Surface patterning on periodicity of femtosecond laser-induced ripples*, Applied Physics Letters **97**(14), 2010, article 141101.

[14] COLOMBIER J.P., GARRELIE F., FAURE N., REYNAUD S., BOUNHALLI M., AUDOUARD E., STOIAN R., PIGEON F., *Effects of electron–phonon coupling and electron diffusion on ripples growth on ultrafast-laser-irradiated metals*, Journal of Applied Physics **111**(2), 2012, article 024902.

[15] COLOMBIER J.P., COMBIS P., ROSENFELD A., HERTEL I.V., AUDOUARD E., STOIAN R., *Optimized energy coupling at ultrafast laser-irradiated metal surfaces by tailoring intensity envelopes: consequences for material removal from Al samples*, Physical Review B **74**(22), 2006, article 224106.

[16] RÖMER G.R.B.E., HUIS IN'T VELD A.J., MEIJER J., GROENENDIJK M.N.W., *On the formation of laser induced self-organizing nanostructures*, CIRP Annals – Manufacturing Technology **58**(1), 2009, pp. 201–204.

[17] VARLAMOVA O., REIF J., VARLAMOV S., BESTEHORN M., *The laser polarization as control parameter in the formation of laser-induced periodic surface structures: comparison of numerical and experimental results*, Applied Surface Science **257**(12), 2011, pp. 5465–5469.

[18] VARLAMOVA O., REIF J., VARLAMOV S., BESTEHORN M., *Modeling of the laser polarization as control parameter in self-organized surface pattern*, Journal of Nanoscience and Nanotechnology **11**(10), 2011, pp. 9274–9281.

[19] QIHONG WU, YURONG MA, RONGCHUAN FANG, YUAN LIAO, QINGXUAN YU, XIANGLI CHEN, KELVIN WANG, *Femtosecond laser-induced periodic surface structure on diamond film*, Applied Physics Letters **82**(11), 2003, pp. 1703–1705.

[20] MIYAJI G., MIYAZAKI K., *Origin of periodicity in nanostructuring on thin film surfaces ablated with femtosecond laser pulses*, Optics Express **16**(20), 2008, pp. 16265–16271.

[21] HONG LIANG, BING SHI, FAIRCHILD A., CALE T., *Applications of plasma coatings in artificial joints: an overview*, Vacuum **73**(3–4), 2004, pp. 317–326.

[22] MARCHETTO D., ROTA A., CALABRI L., GAZZADI G.C., MENOZZI C., VALERI S., *AFM investigation of tribological properties of nano-patterned silicon surface*, Wear **265**(5–6), 2008, pp. 577–582.

[23] YUFEI MO, WENJIE ZHAO, DEMING HUANG, FEI ZHAO, MINGWU BAI, *Nanotribological properties of precision-controlled regular nanotexture on H-passivated Si surface by current-induced local anodic oxidation*, Ultramicroscopy **109**(3), 2009, pp. 247–252.

[24] LITAO QI, NISHII K., NAMBA Y., *Regular subwavelength surface structures induced by femtosecond laser pulses on stainless steel*, Optics Letters **34**(12), 2009, pp. 1846–1848.

[25] WEI ZHANG, GUANGHUA CHENG, QIANG FENG, LAMEI CAO, FENGPING WANG, RONGQING HUI, *Abrupt transition from wavelength structure to subwavelength structure in a single-crystal superalloy induced by femtosecond laser*, Applied Surface Science **257**(9), 2011, pp. 4321–4324.

[26] SAKABE S., HASHIDA M., TOKITA S., NAMBA S., OKAMURO K., *Mechanism for self-formation of periodic grating structures on a metal surface by a femtosecond laser pulse*, Physical Review B **79**(3), 2009, article 033409.

[27] BONCH-BRUEVICH A.M., LIBENSON M.N., MAKIN V.S., TRUBAEV V.V., *Surface electromagnetic waves in optics*, Optical Engineering **31**(4), 1992, pp. 718–730.

*Received December 29, 2011*
*in revised form May 10, 2012*